Supplementary Material

Divergent antibody-mediated population immunity to H5, H7 and H9 subtype potential pandemic influenza viruses

Supplementary Tables

Supplementary Figures

Strain Name	Subtype	Origin	Group	Number of blood donors assessed
A/South Carolina/1/1918	H1	Human	1	337
A/PR/8/1934	H1	Human	1	261
A/USSR/90/1977	H1	Human	1	260
A/Solomon Islands/3/2006	H1	Human	1	253
A/Brisbane/2/2018	H1	Human	1	195
A/England/1/1966	H2	Human	1	202
A/Memphis/1/1968	H3	Human	2	243
A/Udorn/307/1972	H3	Human	2	243
A/Netherlands/233/1982	H3	Human	2	243
A/UK/261/1991	H3	Human	2	243
A/New York/55/2004	H3	Human	2	243
A/South Australia/34/2019	H3	Human	2	243
A/Viet Nam/1204/2004	H5	Human	1	263
A/bar-headed goose/Qinghai/3/2005	H5	Avian	1	512
A/mute swan/England/117298/2022	H5 (2.3.4.4b)	Avian	1	210
A/Texas/37/2024	H5 (2.3.4.4b)	Human	1	N/A
A/New York/107/2003	H7	Human	2	243
A/Shanghai/1/2013	H7	Human	2	243
A/Hong Kong/308/2014	H9	Human	1	209

Table S1: Pseudotyped influenza viruses included in the study, with their corresponding subtype, phylogenetic group, and sample origin. Group 1 (H1, H2 and H5 subtypes) viruses assessed individuals from the same 512-member cohort, whilst Group 2 (H3 and H7 subtypes) viruses assessed individuals from the same 243-member cohort.

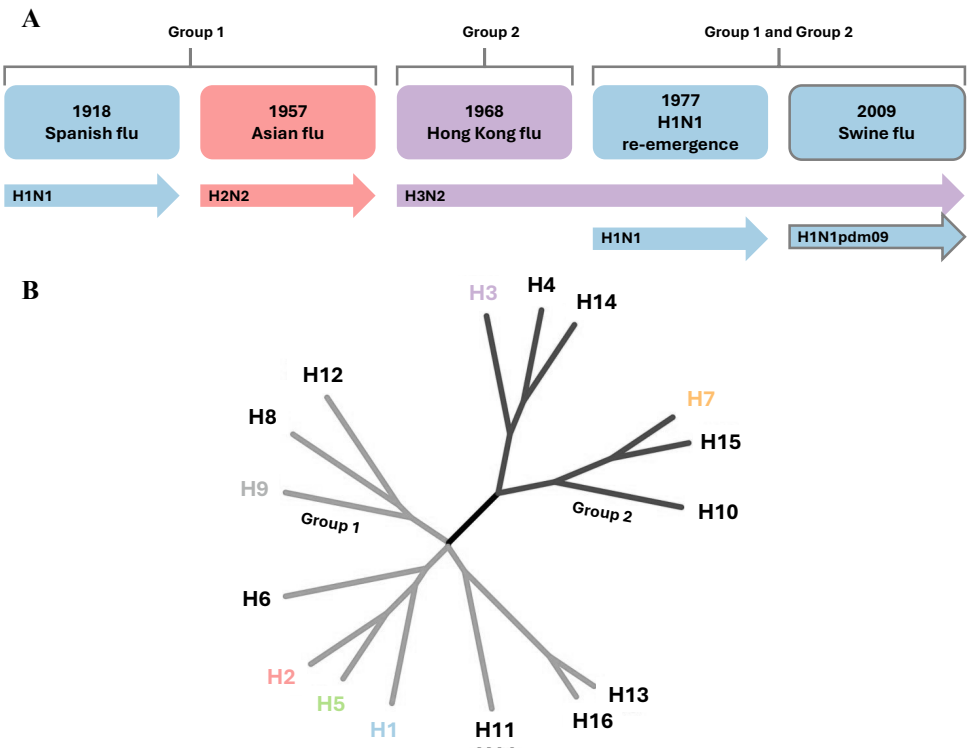

Figure S1: Influenza A circulation timeline and phylogenetic tree. Figure adapted from https://doi.org/10.1073/pnas.0807142105. Group 1 HAs consist of H1, H2, H5, H6, H8, H9, H11, H13 and H16. Group 2 HAs consist of H3, H4, H7, H10, H14 and H15.

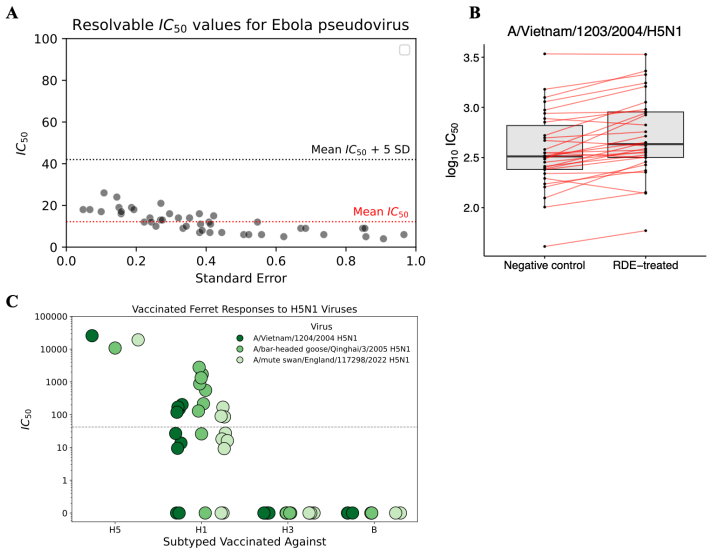

Figure S2: Pseudovirus microneutralisation assay controls. A. Ebola pseudovirus neutralisation assay. 100 sera samples were run against an Ebola pseudovirus, and a seropositivity threshold was determined as five standard deviations above the mean IC_{50}. **B.** Receptor-destroying enzyme assay – 30 sera samples treated with either physiological saline solution or sialic acid-destroying enzyme and used in a neutralisation assay against H5 A/Vietnam/1203/2004 pseudotyped virus. The use of a receptor-destroying enzyme did not remove neutralisation against H5N1; in fact, neutralisation marginally increased. This was statistically significant ($p < 0.001$) according to a paired t-test at a 95% confidence level. **C.** The neutralisation responses of ferrets vaccinated with H1 (n=9), H3 (n=6), H5 (n=1) or Influenza B (n=3) were tested against three H5N1 pseudotyped viruses. Vaccination against H3 or Influenza B did not produce any detectable neutralising antibodies against H5, confirming low assay background. Neutralising antibody responses were greatest in ferrets vaccinated against H5, as expected, with the highest neutralising response against the A/Vietnam/1203/2004 pseudotyped virus that the ferret was specifically vaccinated against. H1 vaccinated ferrets showed detectable neutralising antibodies against H5, that must be due to cross-reactive epitopes between H1 and H5 rather than inherent cross-reactive properties of ferret sera or assay background.

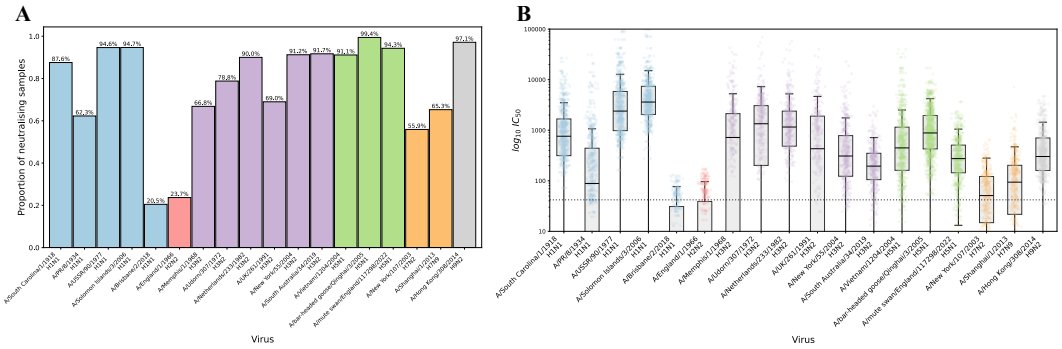

Figure S3: Detectable neutralisation and corresponding IC_{50}s against all tested seasonal and potential pandemic viruses. A. Proportion of neutralising samples for each virus, determined using the seropositivity threshold calculated from the Ebola pseudovirus neutralisation assay (Supplementary Figure 2A). **B.** Corresponding IC_{50}s for each virus. Group 1 and Group 2 viruses were run against different sera sample sets from the 2020 blood donor cohort due to sera quantities available.

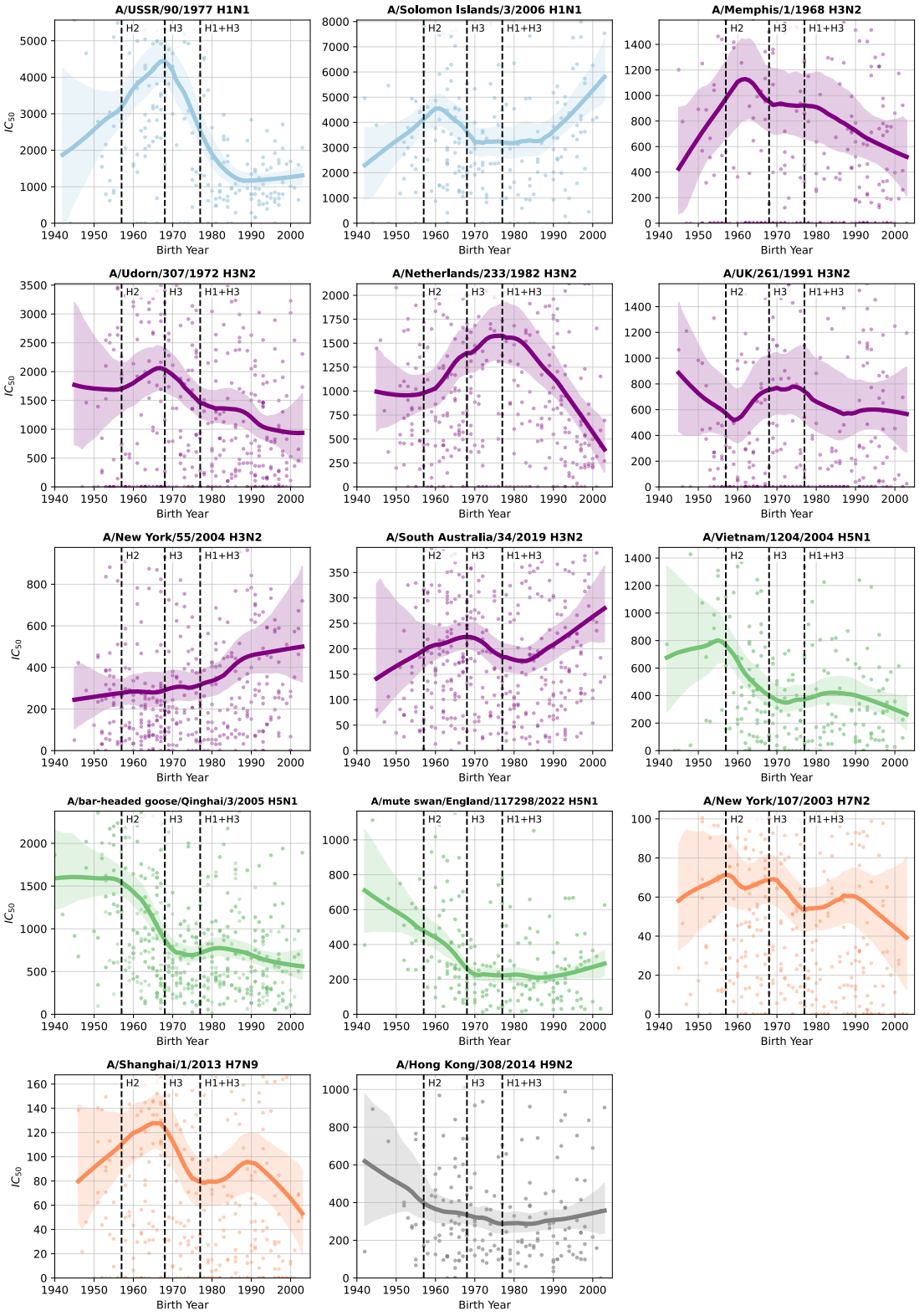

Figure S4: LOWESS trendlines with bootstrapped 95% confidence intervals for the tested potential pandemic and seasonal influenza strains. A smoothing parameter of 0.4 was used.

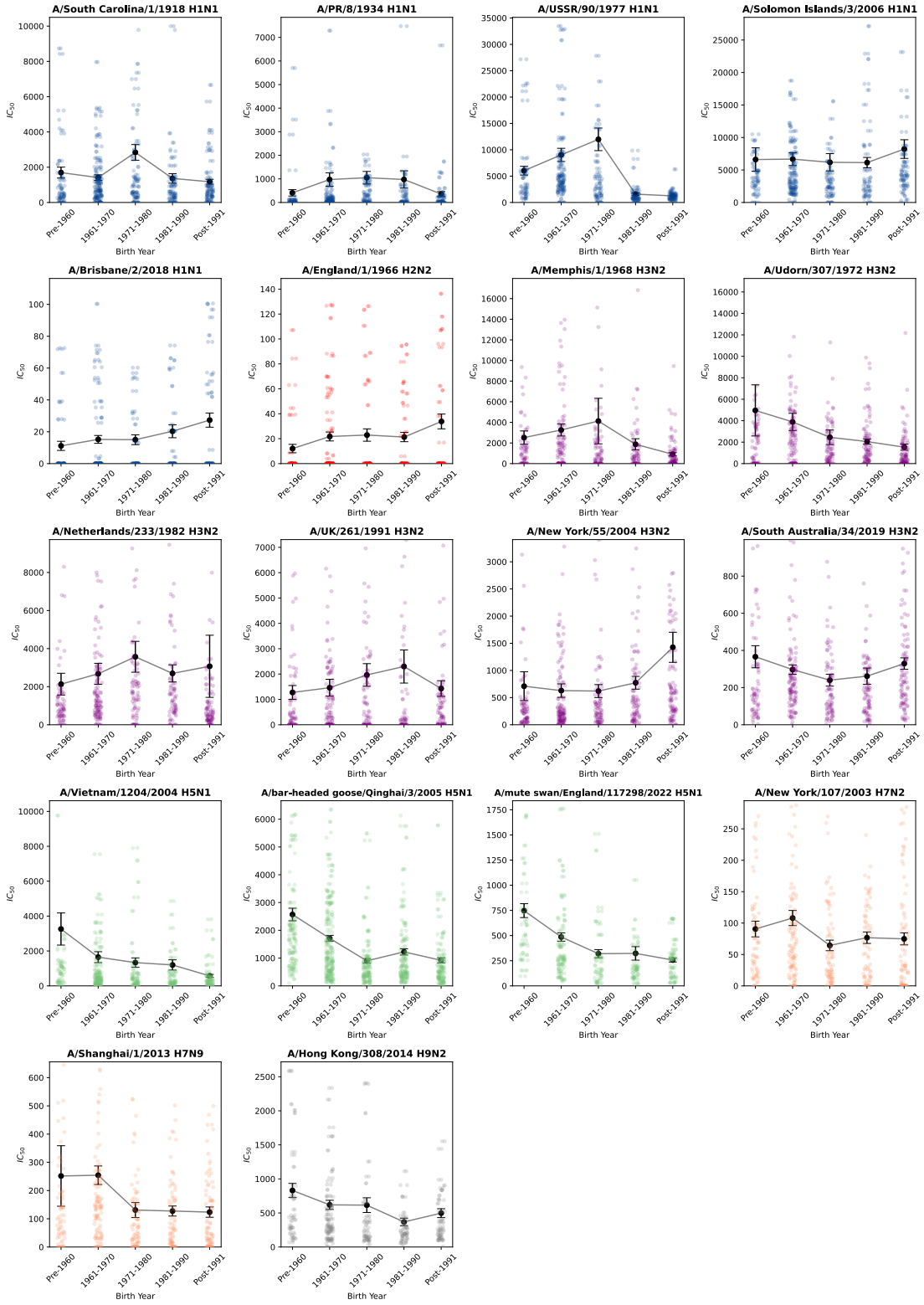

Figure S5: Antibody-mediated immune profiles for all tested influenza strains separated into 10-year age cohorts. The mean IC_{50} and standard error of the mean (SEM) were calculated for each age cohort.

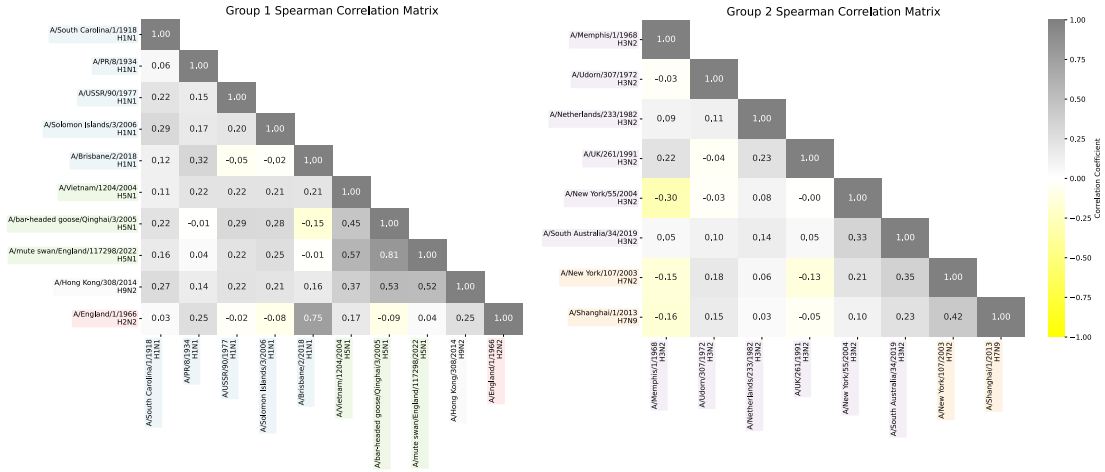

Figure S6: Immune profiles of blood donors indicate that neutralisation of one potential pandemic strain is positively associated with neutralisation of other potential pandemic strains. Associations were assessed using Spearman's correlation for each virus pair.

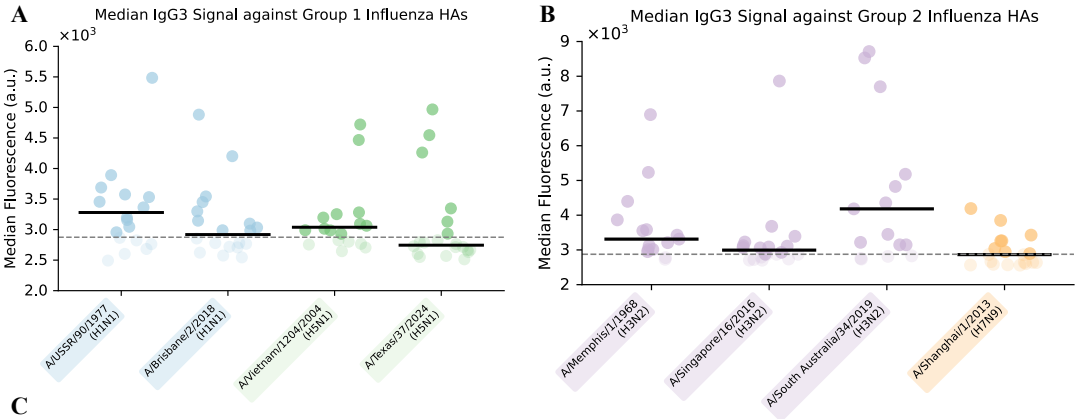

C

Antibody	Negative Threshold (a.u.)
BV421-*anti*-IgG1	1942.74
PE-*anti*-IgG2	3110.23
R718-*anti*-IgG3	2874.98
FITC-*anti*-IgG4	5028.56

Figure S7: Flow cytometry analysis (supplementary material). A. IgG3 Group 1 data (zoomed view). **B.** IgG3 Group 2 data (zoomed view). **C.** Negative threshold values for each IgG.

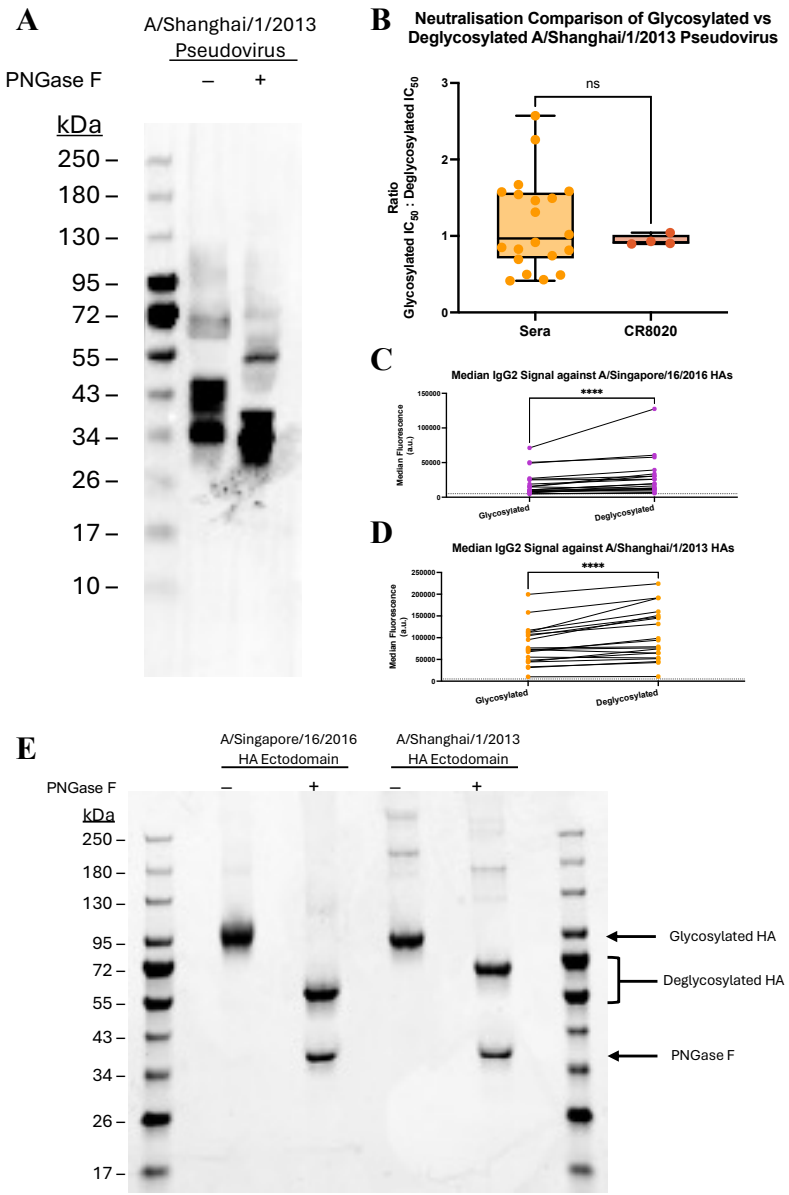

Figure S8: Effects of deglycosylating HAs or pseudotyped viruses using PNGase results. **A** Western Blot band shift showing the effect of deglycosylation on the pseudovirus of A/Shanghai/1/2013. Deglycosylation alters the electrophoretic mobility of HA proteins in polyacrylamide gels by reducing their apparent molecular weight. Accordingly, the PNGase F-treated pseudovirus exhibited a gel shift, migrating further compared to the untreated pseudovirus. A polyclonal primary antibody produced in rabbit (Invitrogen, #PA5-81736) was used. **B.** Effect of glycosylation on the neutralisation of the A/Shanghai/1/2013 pseudovirus. Difference measured by ratio of IC_{50} neutralisation against the glycosylated pseudovirus to the deglycosylated pseudovirus (n=20), when compared to the equivalent ratio achieved by the control antibody, CR8020. Data were not normally distributed; statistical significance was assessed using a non-parametric Kolmogorov–Smirnov test at a 95% confidence interval. **C-D.** Median IgG2 responses for all samples (n=20) across glycosylated and deglycosylated viral HA baits. The data were not normally distributed, so a Wilcoxon matched-pairs signed rank test was performed at a 95% confidence interval. **E.** SDS-PAGE gel shift showing the effect of deglycosylation on A/Singapore/16/2016 and A/Shanghai/1/2013 HA proteins. Deglycosylation alters the migration of HA proteins through a polyacrylamide gel, reflecting changes in molecular weight.

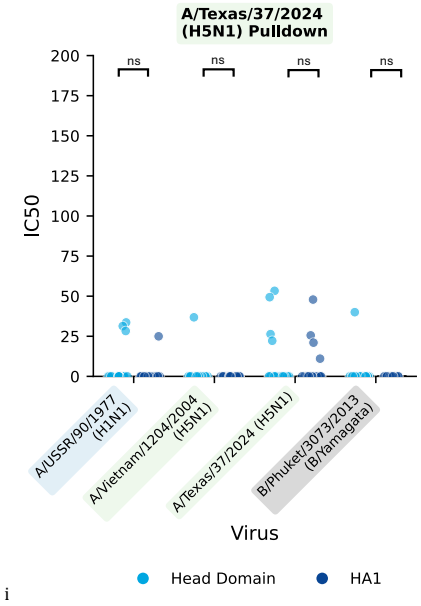

i

Figure S9: Comparison of head domain and HA1 A/Texas/37/2024 proteins. No statistically significant differences were observed between the head domain or the HA1 proteins. Statistical analysis was performed using Mann–Whitney U tests with Holm–Bonferroni correction at a 95% confidence level. Asterisks denote statistical significance: $p < 0.05$ (*), $p < 0.01$ (**), $p < 0.001$ (***).

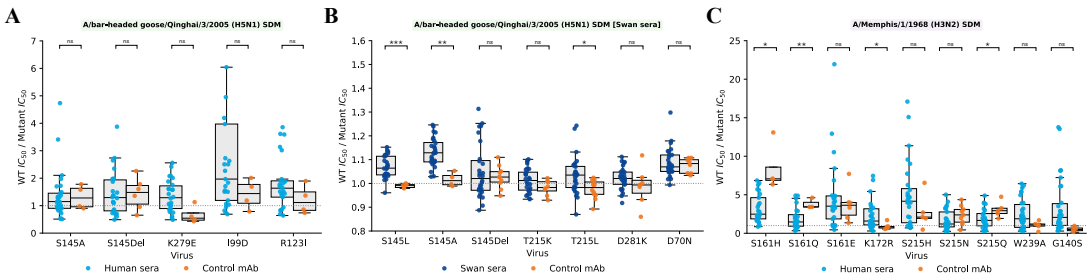

Figure S10: Site-directed mutagenesis of additional H5 and H3 residues, and H5 neutralisation by swan sera. A. Additional H5 mutations. **B.** H5 mutations tested using sera from swans naturally infected with H5N1. **C.** Additional H3 mutations. Statistical analysis was performed using Student's t-tests with Holm-Bonferroni correction on the $\log_{10}$ of the ratios at a 95% confidence level. Asterisks denote statistical significance: $p < 0.05$ (*), $p < 0.01$ (**), $p < 0.001$ (***).